Enhanced wound healing associated with Sharpey's fiber-like tissue formation around FGF-2-apatite composite layers on percutaneous titanium screws in rabbits

Hirotaka Mutsuzaki[1, 2*], Atsuo Ito[2], Yu Sogo[2], Masataka Sakane[3], Ayako Oyane[4], and Naoyuki Ochiai[3]

[1]Department of Orthopaedic Surgery, Ibaraki Prefectural University of Health Sciences, 4669-2 Ami, Ami-machi, Inashiki-gun, Ibaraki 300-0394, Japan

[2]Human Technology Research Institute, National Institute of Advanced Industrial Science and Technology, Central 6, 1-1-1 Higashi, Tsukuba, Ibaraki 305-8566, Japan

[3]Department of Orthopaedic Surgery, Institute of Clinical Medicine, Graduate School of Comprehensive Human Sciences, University of Tsukuba, 1-1-1 Tennodai, Tsukuba, Ibaraki 305-8575, Japan

[4]Nanosystem Research Institute, National Institute of Advanced Industrial Science and Technology, Central 4, 1-1-1 Higashi, Tsukuba, Ibaraki 305-8562, Japan

[*]Corresponding author

Abstract

Background Pin-tract infections are the most common complications of external fixation. To solve the problem, we developed a fibroblast growth factor-2 (FGF-2)-apatite composite layer for coating titanium screws. The purpose of this study was to elucidate the mechanism of the improvement in infection resistance associated with FGF-2-apatite composite layers.

Method We analyzed FGF-2 release from the FGF-2-apatite composite layer and the mitogenic activity of the FGF- 2-apatite composite layer. We evaluated time-dependent development of macroscopic pin-tract infection around uncoated titanium control screws (n = 10). Screws coated with the apatite layer (n = 16) and FGF-2-apatite composite layer (n = 16) were percutaneously implanted for 4 weeks in the medial proximal tibia in rabbits.

Results A FGF-2-apatite composite layer coated on the screws led to the retention of the mitogenic activity of FGF- 2. FGF-2 was released from the FGF-2-apatite composite layer in vitro for at least 4 days, which corresponds to a period when 30% of pin-tract infections develop macroscopically in the percutaneous implantation of uncoated titanium control screws. The macroscopic infection rate increased with time, reaching a plateau of 80–90% within 12 days. This value remained unchanged until 4 weeks after

implantation. The screws coated with an FGF-2-apatite composite layer showed a significantly higher wound healing rate than those coated with an apatite layer (31.25 vs. 6.25%, $p < 0.05$). The interfacial soft tissue that bonded to the FGF-2-apatite composite layer is a Sharpey's fiber-like tissue, where collagen fibers are inclined at angles from 30 to 40° to the screw surface. The Sharpey's fiber-like tissue is rich in blood vessels and directly bonds to the FGF-2- apatite composite layer via a thin cell monolayer (0.8–1.7 _m thick).

Conclusion It is suggested that the enhanced wound healing associated with the formation of Sharpey's fiber-like tissue triggered by FGF-2 released from the FGF-2-apatite composite layer leads to the reduction in the pin-tract inflammation rate.

Keywords

Calcium phosphate coating · External fixation · Fibroblast growth factor-2 · Infection · Sharpey's fibers

Introduction

Pin-tract infections are the most common complications of external fixation [1-6]. To solve this problem, we developed a fibroblast growth factor-2 (FGF-2)-apatite composite layer for coating anodically oxidized titanium screws using a supersaturated calcium phosphate solution supplemented with FGF-2 [7, 8]. Because FGF-2 enhanced wound healing owing to fibroblast proliferation and vascularization [9-16]. The titanium screws coated with an FGF-2-apatite composite layer demonstrated a marked reduction in the rate of macroscopic pin-tract infection compared with titanium screws without the FGF-2-apatite composite layer on a rabbit percutaneous screw implantation model. The rates of infection associated with macroscopic tissue destruction 4 weeks after the implantation were 43.8% for the screws coated with the FGF-2-apatite composite layer and 93.8% for those without the FGF-2-apatite composite layer [7]. The FGF-2-apatite composite layers consisted of low-crystallinity apatite and approximately 2.3 μg of FGF-2 per screw 4.0 mm diameter and 30 mm length.

Since FGF-2 promotes fibroblast proliferation and wound healing with vascularization [9-16], it is hypothesized that FGF-2 is released from the FGF-2-apatite composite layer, and then this released FGF-2 facilitates fibroblast proliferation and angiogenesis which compete with the spread of infection; finally, the pin-tract infection

is prevented or cured by improved skin wound healing. Moreover, we considered that an anchoring formation between the pin and skin wound is important in order to prevent the pin-tract infection. Sharpey's fibers are a highly infection-resistant percutaneous structure owing to its periodontal membrane [17]. Sharpey's fibers in the periodontal membrane bridge the tooth surface and the bone surface. They are aligned perpendicular or inclined to the tooth and bone surfaces with blood vessels and nerves running in the interstices of the fibers. They are embedded in bone on one side and in radicular cementum on the other side. The blood vessels in the interstices of Sharpey's fibers supply immunological cells that remove bacteria infected through the interface between the tooth surface and the gingival tissue. Therefore, we hypothesized that Sharpey's fiber-like tissue formation can be related to the marked increase in infection resistance. However, the detailed mechanism of the improved infection resistance remains unclear for the following reasons: Firstly, only limited information is available about the release profile of FGF-2. Secondly, no information is available about how FGF-2-mediated tissue regeneration competes with the development of infection-mediated tissue destruction. Thirdly and most importantly, no information is available about inflammation and soft tissue reactions to FGF-2-apatite composite layers at the histological level. In our previous study, infection resistance was not evaluated in

histological detail but only macroscopically. The purpose of the present study was, therefore, to elucidate the mechanism of the improvement in infection resistance associated with FGF-2-apatite composite layers with particular focus on the above three issues.

Materials and Methods

Formation of FGF-2-apatite composite layer on titanium screws

Titanium cancellous screws with a 142-nm-thick anodic oxide layer (SYNTHES®, USA) (# 407-030, 4.0 mm diameter and 30 mm length) were coated with an apatite layer and an FGF-2-apatite composite layer [7, 8]. Briefly, titanium cancellous screws were immersed for 48 h in a supersaturated calcium phosphate solution (Table 1) with a Ca/P molar ratio of 2.0 at neutral pH at 37 ºC. Each supersaturated calcium phosphate solution (10 ml) was prepared by mixing 5 clinically available infusion fluids in Japan at a certain mixing ratio: Ringer's solution (8.137 ml, Otsuka Pharmaceutical Co., Ltd., Japan) and Calcium Chloride Corrective Injection 1 mEq/ml (36.85 µl, Otsuka Pharmaceutical Co., Ltd., Japan) as calcium sources, Klinisalz (0.899 ml, I'rom Pharmaceutical Co., Ltd., Japan) and Dipotassium Phosphate Corrective Injection 1 mEq/ml (18.72 µl, Otsuka Pharmaceutical Co., Ltd., Japan) as

105 phosphorus sources, and Sodium Bicarbonate Substitution Fluid for only BIFIL®
106 (0.909 ml, AJINOMOTO PHARMACEUTICALS Co., Ltd., Japan) as an alkalinizer.
107 Therefore, the supersaturated calcium phosphate solution had fixed chemical
108 composition. The supersaturated calcium phosphate solutions contained FGF-2
109 (Fiblast®, Kaken Pharmaceutical, Japan) at a concentration of 0 or 4 μg/ml. The screws
110 immersed in the supersaturated calcium phosphate solutions with FGF-2 concentrations
111 of 0 and 4 μg/ml were designated as F0 and F4 screws, respectively. F0 and F4 have the
112 almost same surface morphology and the surface layer on both samples mainly
113 consisted of low-crystalline apatite [7]. So using these two samples, only the effect of
114 immobilized FGF-2 in the surface layer should be examined without interference caused
115 by difference in surface properties. The composition was not actually measured on the
116 screw surface.
117
118 *In vitro FGF-2 release from FGF-2-apatite composite layer*
119 The F4 screw was rinsed with 1 ml of physiological saline solution, and then
120 immersed in 1 ml of fresh physiological saline solution at 37 ºC (n = 6). The
121 physiological saline solution was replaced with a fresh solution every day for 4 days.
122 The saline solution was analyzed for FGF-2 by fluorometric quantification (excitation

123 wavelength: 470 nm, emission wavelength: 570 nm) using a NanoOrange® Protein
124 Quantitation Kit (N-6666, Invitrogen, USA) in accordance with the manufacturer's
125 instructions. The working curve was drawn normally similar to one in the instructions
126 (data not shown).
127
128 *In vitro assay for mitogenic activity of FGF-2-apatite composite layer*
129 Fibroblastic NIH3T3 cells (NIH3T3-3-4, RIKEN BioResource Center) were
130 cultured on the F0 and F4 screws to evaluate the mitogenic activity of the apatite layer
131 and FGF-2-apatite composite layer. The cells on the screws were cultured in 5 mL of
132 Dulbecco's modified essential medium supplemented with 0.3 mg/ml l-glutamine, 1.0
133 mg/ml bovine serum albumin, 5.0 μg/ml insulin and 1.0 μg/ml transferrin (serum-free
134 DMEM) in a humidified atmosphere of 5% CO_2 at 37 ºC. Since serum contains various
135 growth factors and other biologically active substances, serum-free DMEM was used to
136 detect the effect of immobilized FGF-2 on the titanium screw (F4). BSA, insulin and
137 transferrin were added to DMEM as minimum requirement additives for survival of the
138 cells under the condition without serum. The absorbance of serum-free DMEM at 450
139 nm (n = 6) were measured every day for 6 days using a water-soluble tetrazolium salt
140 (the CCK-8 kit, Dojindo Laboratories, Japan); each screw with cells was incubated in 1

ml of fresh and 10% tetrazolium salt-containing serum-free DMEM to determine the absorbance at 450 nm instead of cell numbers on the screws. After the incubation with CCK-8 reagent, the screws were rinsed and re-immersed in the original 5 ml of serum-free DMEM for cell incubation in a humidified atmosphere of 5% CO_2 at 37 ºC until the next measurement. It is confirmed that the number of the cells is proportional to the measured Abs (450 nm) under this experimental condition in advance (data not shown).

In vivo study

The F0 and F4 screws were implanted percutaneously in the medial proximal tibia of sixteen skeletally mature male Japanese white rabbits weighing approximately 3.0 kg. The operation technique was the same as that of our previous works [7, 8]. Briefly, the screws were implanted in both medial proximal tibiae of eight rabbits in each group (F0 and F4) after the intravenous injection of barbiturate (40 mg/kg body weight), a small (10 mm) incision in the skin on the medial proximal tibia and a perforation 2.5 mm in diameter in both tibial metaphysises using individual taps. After the implantation, the skin was sutured bilaterally to the screw [7, 8]. Postoperatively, each rabbit was allowed to behave freely in its own cage. The rabbits did not receive

any antibiotics or treatment for their wounds and were sacrificed 4 weeks after the operation.

Using the same operation techniques, ten uncoated titanium control screws were implanted percutaneously in both medial proximal tibiae of five skeletally mature male Japanese white rabbits weighing approximately 3.0 kg to evaluate the natural development of pin-tract infection using a Kaplan-Meier plot. Pin-tract infection was macroscopically examined once a day for four weeks. All the animal experiments were performed in accordance with the guidelines of the Ethical Committee of the University of Tsukuba, National Institute of Advanced Industrial Science and Technology and the National Institute of Health guidelines for the care and use of laboratory animals (NIH Pub. No. 85-23 Rev. 1985).

Histological evaluation of pin-tract inflammation around F0 and F4 screws

After extracting the F0 and F4 screws, soft tissues at the screw site (F0: n = 16, F4: n = 16) were fixed in 10% neutral-buffered formalin and embedded in paraffin. Sections were cut at the center of the screw hole parallel to the screw hole and sliced to a thickness of 5 μm. The sections were stained with hematoxylin and eosin (H&E) and by Von Kossa's method and Masson's trichrome (MT) method for histological

177 evaluation by light microscopy (BX-51, Olympus Optical Co., Ltd., Japan). Von Kossa's
178 and MT methods were used for detecting the FGF-2-apatite composite layer and
179 collagen fibers, respectively.

180 Pin-tract inflammation was histologically assessed in a blind manner by a
181 single pathologist by classifying it into one of three grades (Grades 0, 1 and 2). Grade 0
182 corresponds to "no inflammation with good wound healing". Grade 1 corresponds to
183 "slight inflammation". Grade 2 corresponds to "severe inflammation". The alignment of
184 collagenous fibers at the tissue-screw interface in specimens with Grade 0 inflammation
185 was examined by polarized light microscopy (BH-2, Olympus Optical Co., Ltd., Japan).

186

187 *Evaluation of time-dependent development of macroscopic pin-tract infection around*
188 *uncoated titanium control screws*

189 The development of pin-tract infection around uncoated titanium control
190 screws was macroscopically evaluated once a day using a modified Checketts and
191 Otterburn classification method, adopting the same criteria as those described elsewhere
192 [7]. Briefly, Grade 0 corresponds to "no redness," in which no redness, discharge or
193 screw loosening is observed. Grade 1 corresponds to infections only in the soft tissue,
194 characterized by redness and discharge around the screw without screw loosening.

195 Grade 2 corresponds to infections in both soft and hard tissues, characterized by redness
196 and discharge around the screw associated with screw loosening due to osteomyelitis.
197 Grade 0 survival was determined by the Kaplan-Meier method [18] using Grades 1 and
198 2 described above as end points.
199 Those experiments were summarized in Table 2.
200
201 *Statistical Analyses*
202 The cell proliferation data of the F0 and F4 screw groups were analyzed using
203 Student's *t*-test at a $p < 0.05$ significance level. The pin-tract inflammation grades of the
204 F0 and F4 screw groups were compared using Mann-Whitney's U test at a $p < 0.05$
205 significance level.
206
207 ***Results***
208 *In vitro FGF-2 release from FGF-2-apatite composite layer*
209 FGF-2 was released from the F4 screw for at least 4 days when the screws
210 were immersed in saline solution. 50 to 85 ng of FGF-2 was released from the F4 screw
211 every day during the 4 day immersion (Fig. 1).
212

In vitro assay for mitogenic activity of FGF-2-apatite composite layer

It was confirmed that the FGF-2-apatite composite layer retained the mitogenic activity of FGF-2 *in vitro* (Fig. 2). No significant difference was detected between the initial numbers of NIH3T3 cells adhering to the F0 and F4 screws. Therefore, the apatite layer and FGF-2 apatite composite layer were the same in terms of cell adhesiveness. Nevertheless, after 3 and 4 day incubations, the absorption intensities of metabolized tetrazolium salt in the serum-free DMEM became significantly higher for the F4 screws than that for the F0 screws. This result suggested that the number of cells on the F4 screws became significantly higher than that on the F0 screws.

Development of macroscopic pin-tract infection around uncoated titanium control screw

The macroscopic infection rate for uncoated titanium control screws reached 30% in the initial period between 2 and 4 days after implantation, which was demonstrated by Grade 0 survival in the Kaplan-Meier plot (Fig. 3). The macroscopic infection rate increased with increasing implantation period, reaching a plateau of 80-90% within 12 days. This value remained unchanged until 4 weeks after implantation. The final infection rate was consistent with that in our previous study [7].

Histological evaluation of pin-tract inflammation around F0 and F4 screws

In the F0 screw group, the rates of Grade 0, 1 and 2 inflammation were 1/16 (6.25%), 6/16 (37.5%) and 9/16 (56.25%), whereas in the F4 screw group the rates of Grade 0, 1 and 2 inflammation were 5/16 (31.25%), 7/16 (43.75%) and 4/16 (25.0%), respectively (Fig. 4). The F4 screws demonstrated a significant improvement in wound healing without inflammation compared with the F0 screws, which was demonstrated by the significant difference in the rate of Grade 0 inflammation between the F0 and F4 screw groups ($p = 0.018$) (Fig. 5).

Sharpey's fiber-like tissue with blood vessels was found to have formed around two of the five F4 screws in the case of Grade 0 inflammation. In one F4 specimen with Grade 0 inflammation where the screw-skin interface was completely intact (Fig. 6a), an extraordinary interfacial tissue with a thickness of 100 μm was found to have formed on the FGF-2-apatite composite layer. The interfacial tissue consisted of an inner cell monolayer and an outer fibrous tissue layer attached to the inner cell monolayer. The inner cell monolayer consisted of extremely thin and stretched cells (0.8-1.7 μm thick and 16-33 μm long) (Fig. 6b). The inner cell monolayer directly attached to the FGF-2-apatite composite layer (Fig. 7). In the outer fibrous tissue layer,

many blood vessels were formed. Polarized light microscopy demonstrated the interference color (light gray) in the outer fibrous tissue layer with 4-fold color extinction during 360° sample rotation under crossed polar observation (Figs. 6c and d). This meant that collagen fibers ran in one direction. The running direction of the collagen fibers was not parallel to the screw surface but inclined at angles from 30 to 40°, which was demonstrated by the angle between the extinction position and the screw hole direction at the extinction position (Figs. 6c and d). These morphological features of the outer fibrous tissue layer have close similarity to those of Sharpey's fibers in the periodontal membrane. In the interstices of the slanted collagen fibers, flattened fibroblasts were sparsely present, and aligned parallel to the collagen fibers. The cell sparseness indicated that the intensive formation of an extracellular matrix including collagen occurred. In another F4 specimen with Grade 0 inflammation where the screw-skin interface was incompletely intact, Sharpey's fiber-like tissue with many blood vessels was again observed. In the other (three) F4 specimens with Grade 0 inflammation, the formation of Sharpey's fiber-like tissue was not confirmed owing to the rupture of soft tissue on the removal of the screws. On the other hand, the formation of Sharpey's fiber-like tissue was not confirmed in the only F0 specimen with Grade 0 inflammation (Fig. 8).

Discussion

FGF-2 was released from the F4 screws for at least 4 days *in vitro*. FGF-2 released from the apatite layer retained its bioactivity and triggered the proliferation of NIH3T3 cells for 4 days. On the other hand, most of the pin-tract infections in the case of the uncoated titanium control screws occurred within 12 days, with one-third of them occurring within 4 days (Fig. 3). Wound healing proceeds in the gap between the skin and the uncoated titanium control screws. However, bacteria can easily infect in the gap because the anchoring between the skin and the screws remains loose in the early postoperative period. Therefore, the initial competition of wound healing against the spread of infection is crucial for improving infection resistance. On the basis of these results, it is considered that FGF-2 released in the early postoperative period affected wound healing so that it prevailed over the spread of infection. It was suggested that FGF-2 released from the FGF-2-apatite composite layer facilitated fibroblast proliferation and wound healing in the early postoperative period, and that this initial effect of the FGF-2-apatite composite layer was crucial for preventing pin tract infection up to 4 weeks.

The enhanced wound healing triggered by FGF-2 finally led to the reduction

285 in the pin-tract inflammation rate. The F4 screws showed a significantly lower
286 inflammation rate (68.75% vs 93.75%) than the F0 screws in the histological evaluation.
287 FGF-2 released from the FGF-2-apatite composite layer can promote the regeneration of
288 skin tissue and blood vessels. Moreover, apatite has a good affinity with soft-tissue [19,
289 20]. Although the F4 screw reduced pin-tract inflammation rate in the present animal
290 model without using antibiotics and daily pin care routine, the infection rate was still as
291 high as 68.75%. To reduce further the inflammation rate, it is necessary to use
292 antibiotics and daily pin care routine. External fixation pins coated with FGF-2-apatite
293 composite layers needs to be in combination with antibiotics and daily pin care routine
294 to prevent inflammation completely.

295 The induction of Sharpey's fiber-like tissue is related to the marked increase
296 in infection resistance. Sharpey's fibers are present in the periodontal membrane and
297 bone-tendon junctions, which are subjected to transversal and shear stresses [17, 21-23].
298 It should be noted that a tooth, which is a natural percutaneous structure, is a highly
299 infection-resistant percutaneous structure owing to its periodontal membrane. In the
300 present study, the enhanced wound healing was associated with the formation of an
301 extraordinary interfacial tissue that contains Sharpey's fiber-like tissue, where its
302 collagen fibers are inclined to the screw surface at angles from 30 to 40°. Usually,

collagen fibers align parallel to the surface of a foreign body, forming a fibrous connective tissue. An ordinary fibrous connective tissue that aligns parallel to the surface of a foreign body has no blood vessels or nerves.

Whether one end of the collagen fibers in the present Sharpey's fiber-like tissue is embedded in the FGF-2-apatite composite layer remains to be clarified. The Sharpey's fiber-like tissue directly bonded to the cell monolayer. Moreover, no intervening tissues were microscopically observed between the cell monolayer and the FGF-2-apatite composite layer. However, it is unclear whether the Sharpey's fiber-like tissue penetrates the thin cell monolayer. Further ultrastructural studies are required to clarify this.

FGF-2 administered in alveolar bone defects has been shown to enhance the regeneration of the periodontal membrane with new cementum deposits and new bone formation without epithelial downgrowth 6 to 8 weeks after surgery in a dog model [24, 25]. In addition, the regeneration of the periodontal membrane and tendon-bone attachment with Sharpey's fiber was reported [26-29]. External fixation screws with the FGF-2-apatite composite layer in skin tissue resemble an FGF-2-administered natural tooth in the periodontal tissue in that both have the surface apatite layer and FGF-2, have one end immersed in bone marrow that can supply mesenchymal stem cells for

tissue induction or regeneration, and are subjected to transversal and shear stresses. Probably owing to these environmental similarities, FGF-2 released from the FGF-2-apatite composite layer promoted wound healing associated with the formation of Sharpey's fiber-like tissue with blood vessels.

Clinically, the improvement of wound healing of screw-skin interfaces is important in the course of treatment by percutaneous implants such as external fixation. Such implants may also decrease the risk of the inadequate healing of a fractured bone, including nonunion.

In conclusion, titanium screws coated with an FGF-2-apatite composite layer demonstrated the sustained release of FGF-2 for at least 4 days and triggered the enhanced proliferation of fibroblasts in the period. The period was corresponding to the early postoperative phase during which pin-tract infection develops in the percutaneous implantation of uncoated titanium control screws. The skin tissue directly adhered to the FGF-2-apatite composite layer on the screw via a thin cell monolayer. In addition, Sharpey's fiber-like tissue was induced at the screw-skin interface. The Sharpey's fiber-like tissue was rich in blood vessels. All these factors contributed to the remarkable infection resistance associated with the FGF-2-apatite composite layer on titanium external fixation screws. Further studies including ultrastructural analysis at the

339 tissue-apatite composite layer interface, as well as studies entailing long-term
340 implantation and implantation under loaded conditions are required.
341

342 ***References***

343 1. Oh CW, Kim SJ, Park SK, Kim HJ, Kyung HS, Cho HS, Park BC, Ihn JC (2011)
344 Hemicallotasis for correction of varus deformity of the proximal tibia using a unilateral
345 external fixator. J Orthop Sci 16:44-50

346 2. Catagni MA, Lovisetti L, Guerreschi F, Camagni M, Albisetti W, Compagnoni P,
347 Combi A (2010) The external fixation in the treatment of humeral diaphyseal fractures:
348 outcomes of 84 cases. Injury 41:1107-1111

349 3. Lamm BM, Gottlieb HD, Paley D (2010) A two-stage percutaneous approach to
350 charcot diabetic foot reconstruction. J Foot Ankle Surg 49:517-522

351 4. Pieske O, Geleng P, Zaspel J, Piltz S (2008) Titanium alloy pins versus stainless steel
352 pins in external fixation at the wrist: a randomized prospective study. J Trauma
353 64:1275-1280

354 5. Cavusoglu AT, Er MS, Inal S, Ozsoy MH, Dincel VE, Sakaogullari A (2009) Pin site
355 care during circular external fixation using two different protocols. J Orthop Trauma
356 23:724-730

357 6. Savolainen VT, Pajarinen J, Hirvensalo E, Lindahl J (2010) Hybrid external fixation
358 in treatment of proximal tibial fractures: a good outcome in AO/ASIF type-C fractures.
359 Arch Orthop Trauma Surg 130:897-901

360 7. Mutsuzaki H, Ito A, Sakane M, Sogo Y, Oyane A, Ochiai N (2008) FGF-2-apatite
361 composite layers on titanium screws to reduce pin tract infection rate. J Biomed Mater
362 Res B 86:365-374

363 8. Mutsuzaki H, Ito A, Sakane M, Sogo Y, Oyane A, Ebihara Y, Ichinose N, Ochiai N
364 (2007) Calcium phosphate coating formed in infusion fluid mixture to enhance fixation
365 strength of titanium screws. J Mater Sci Mater Med 18:1799-1808

366 9. Bhang SH, Sun AY, Yang HS, Rhim T, Kim DI, Kim BS (2011) Skin regeneration
367 with fibroblast growth factor 2 released from heparin-conjugated fibrin. Biotechnol Lett
368 33:845-851

369 10. Shi C, Chen W, Zhao Y, Chen B, Xiao Z, Wei Z, Hou X, Tang J, Wang Z, Dai J
370 (2011) Regeneration of full-thickness abdominal wall defects in rats using collagen
371 scaffolds loaded with collagen-binding basic fibroblast growth factor. Biomaterials
372 32:753-759

373 11. Cornwell KG, Pins GD (2010) Enhanced proliferation and migration of fibroblasts
374 on the surface of fibroblast growth factor-2-loaded fibrin microthreads. Tissue Eng Part
375 A 16:3669-3677

376 12. Kalghatgi S, Friedman G, Fridman A, Clyne AM (2010) Endothelial cell
377 proliferation is enhanced by low dose non-thermal plasma through fibroblast growth
378 factor-2 release. Ann Biomed Eng 38:748-757

379 13. Hirooka T, Fujiwara Y, Inoue S, Shinkai Y, Yamamoto C, Satoh M, Yasutake A,
380 Eto K, Kaji T (2009) Suppression of fibroblast growth factor-2 expression: possible
381 mechanism underlying methylmercury-induced inhibition of the repair of wounded
382 monolayers of cultured human brain microvascular endothelial cells. J Toxicol Sci
383 34:433-439

384 14. Schultz GS, Wysocki A (2009) Interactions between extracellular matrix and growth
385 factors in wound healing. Wound Repair Regen 17:153-162

386 15. Nurata H, Cemil B, Kurt G, Uçankus NL, Dogulu F, Omeroglu S (2009) The role of
387 fibroblast growth factor-2 in healing the dura mater after inducing cerebrospinal fluid
388 leakage in rats. J Clin Neurosci 16:542-544

16. Xie JL, Bian HN, Qi SH, Chen HD, Li HD, Xu YB, Li TZ, Liu XS, Liang HZ, Xin BR, Huan Y (2008) Basic fibroblast growth factor (bFGF) alleviates the scar of the rabbit ear model in wound healing. Wound Repair Regen 16:576-581

17. Roberts WE, Chamberlain JG (1978) Scanning electron microscopy of the cellular elements of rat periodontal ligament. Arch Oral Biol 23:587-589

18. Kaplan EL, Meier P (1953) Nonparametric estimation from incomplete observations. J Am Stat Assoc 53:457–481

19. Furuzono T, Sonoda K, Tanaka J (2001) A hydroxyapatite coating covalently linked onto a silicone implant material. J Biomed Mater Res 56:9-16

20. Furuzono T, Wang PL, Korematsu A, Miyazaki K, Oido-Mori M, Kowashi Y, Ohura K, Tanaka J, Kishida A (2003) Physical and biological evaluations of sintered hydroxyapatite/silicone composite with covalent bonding for a percutaneous implant material. J Biomed Mater Res B Appl Biomater 65:217-226

21. Cooper RR, Misol S (1970) Tendon and ligament insertion: A light and electron microscopic study. J Bone Joint Surg Am 52:1-21

22. Short E, Johnson RB (1990) Effects of tooth function on adjacent alveolar bone and Sharpey's fibers of the rat periodontium. Anat Rec 227:391-396

406 23. Simmons DJ, Menton DN, Miller S, Lozano R (1993) Periosteal attachment fibers
407 in the rat calvarium. Calcif Tissue Int 53:424-427

408 24. Murakami S, Takayama S, Ikezawa K, Shimabukuro Y, Kitamura M, Nozaki T,
409 Terashima A, Asano T, Okada H (1999) Regeneration of periodontal tissues by basic
410 fibroblast growth factor. J Periodontal Res 34:425-430

411 25. Sato Y, Kikuchi M, Ohata N, Tamura M, Kuboki Y (2004) Enhanced cementum
412 formation in experimentally induced cementum defects of the root surface with the
413 application of recombinant basic fibroblast growth factor in collagen gel in vivo. J
414 Periodontol 75:243-248

415 26. Chen YL, Chen PK, Jeng LB, Huang CS, Yang LC, Chung HY, Chang SC (2008)
416 Periodontal regeneration using ex vivo autologous stem cells engineered to express the
417 BMP-2 gene: an alternative to alveolaplasty. Gene Ther 15:1469-1477

418 27. Camelo M, Nevins ML, Lynch SE, Schenk RK, Simion M, Nevins M (2001)
419 Periodontal regeneration with an autogenous bone-Bio-Oss composite graft and a
420 Bio-Gide membrane. Int J Periodontics Restorative Dent 21:109-119

421 28. Shirakata Y, Taniyama K, Yoshimoto T, Miyamoto M, Takeuchi N, Matsuyama T,
422 Noguchi K (2010) Regenerative effect of basic fibroblast growth factor on periodontal
423 healing in two-wall intrabony defects in dogs. J Clin Periodontol 37:374-381

424 29. Soda Y, Sumen Y, Murakami Y, Ikuta Y, Ochi M (2003) Attachment of autogenous
425 tendon graft to cortical bone is better than to cancellous bone: a mechanical and
426 histological study of MCL reconstruction in rabbits. Acta Orthop Scand 74:322-326

427

Table 1 Concentrations of chemical components in the immersion solutions

	F0	F4
	mM	mM
Na^+	138.87	138.87
K^+	7.39	7.39
Ca^{2+}	3.67	3.67
Mg^{2+}	0.22	0.22
Cl^-	134.39	134.39
$H_2PO_4^-$	0.90	0.90
HPO_4^{2-}	0.94	0.94
HCO_3^-	15.09	15.09
CH_3COO^-	1.80	1.80
xylitol	29.93	29.93
	μg/mL	μg/mL
FGF-2	0.0	4.0

Table 2 Experiments list			
In vitro study	FGF-2 release from FGF-2-apatite composite layer	F4 screw	Fig. 1
	In vitro assay for mitogenic activity of FGF-2-apatite composite layer	F4 and F0 screw	Fig. 2
In vivo study	Evaluation of time-dependent development of macroscopic pin-tract infection	Uncoated titanium control screw	Fig. 3
	Histological evaluation of pin-tract inflammation	F4 and F0 screw	Fig. 4, 5, 6, 7, 8

Figure

Figure 1.

Cumulative release of FGF-2 from FGF-2-apatite composite layer *in vitro*.

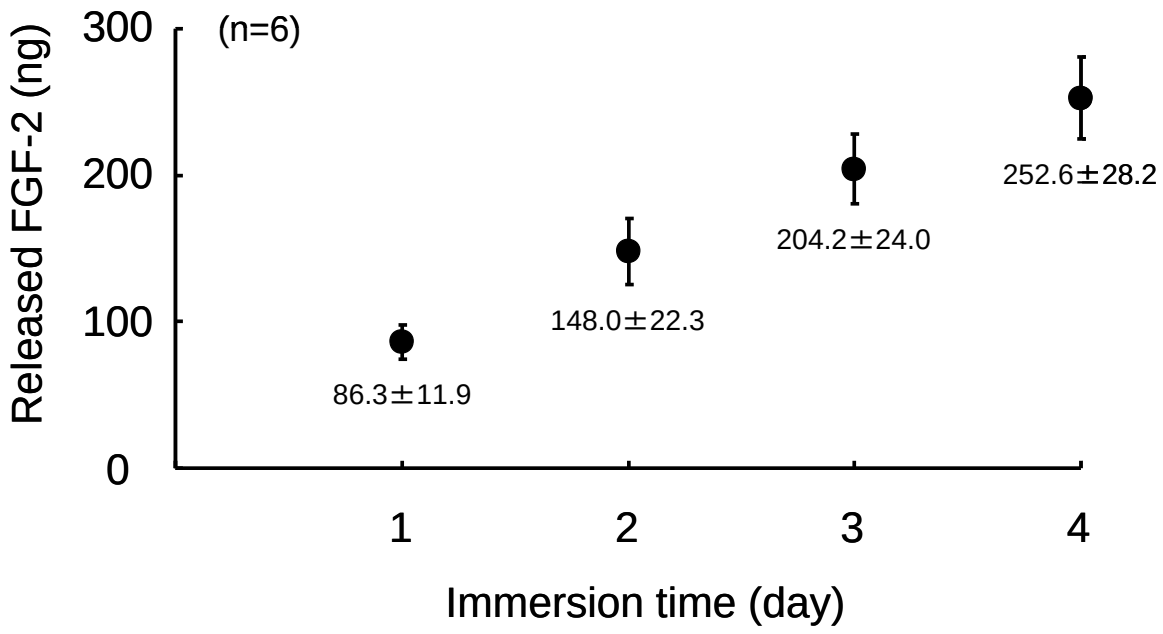

Figure 2.

The change in absorbance of 10% tetrazolium salt-containing serum-free DMEM at 450 nm after 1-hour incubation with NIH3T3 cells that were incubated on F0 and F4 for 0 to 6 days.

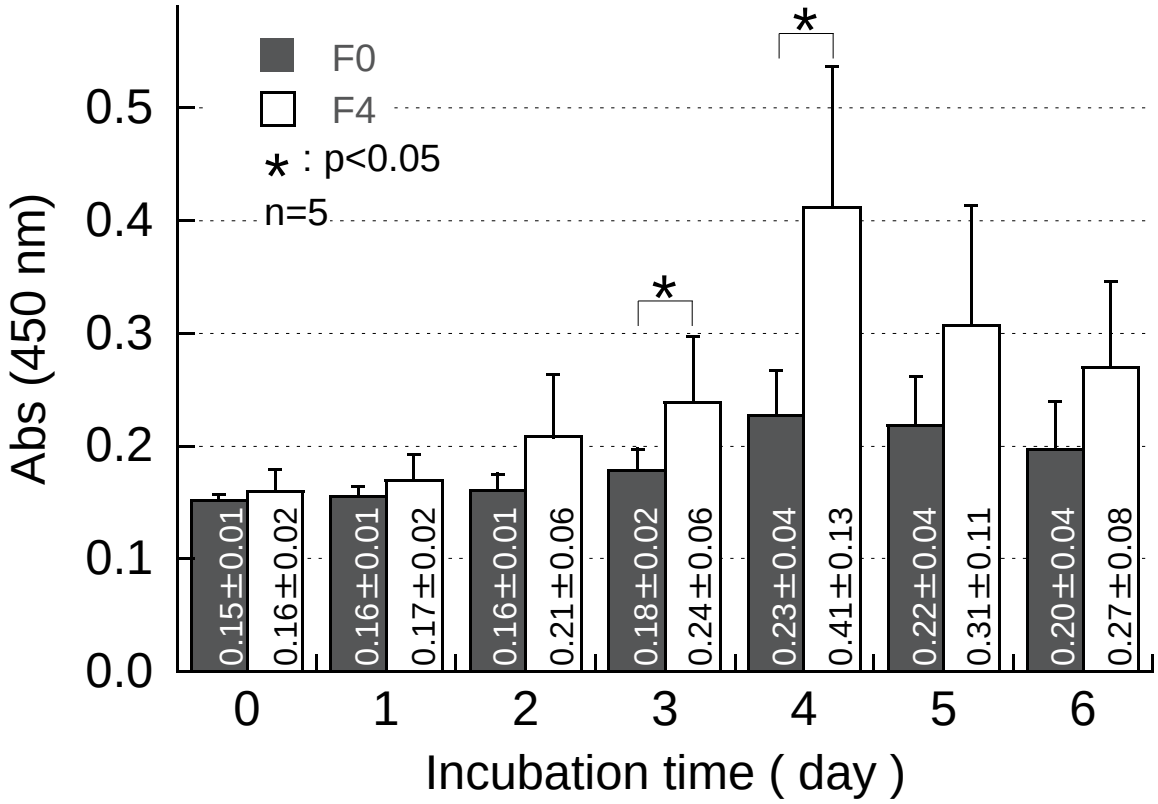

Figure 3.

Time-dependent development of macroscopic pin-tract infection around uncoated titanium control screw.

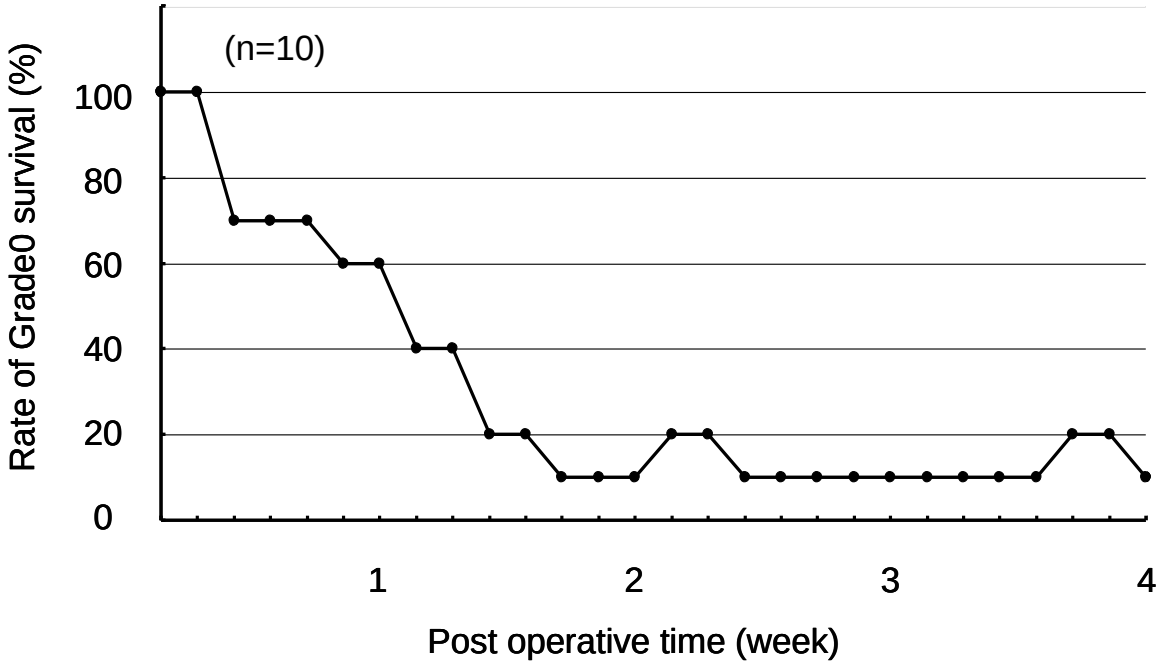

Figure 4.

Typical examples of Grade 0, 1 and 2 inflammation 4 weeks after operation.

Arrows: contact area with screw.

Grade 0: no inflammation with good wound healing (white arrows) (Fig. 4a).

Grade 1: slight inflammation (gray arrows) (Fig. 4b).

Grade 2: severe inflammation (black arrows) (Fig. 4c).

(a)

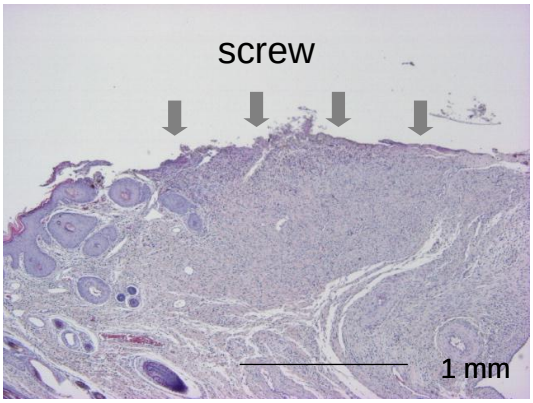

(b)

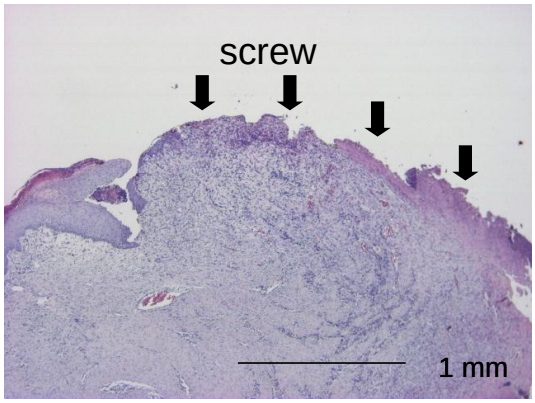

(c)

Figure 5.

Histological evaluation of pin-tract inflammation around F0 and F4 screws.

The inflammation around the F4 screw was significantly less prominent than that around the F0 screw ($p = 0.018$).

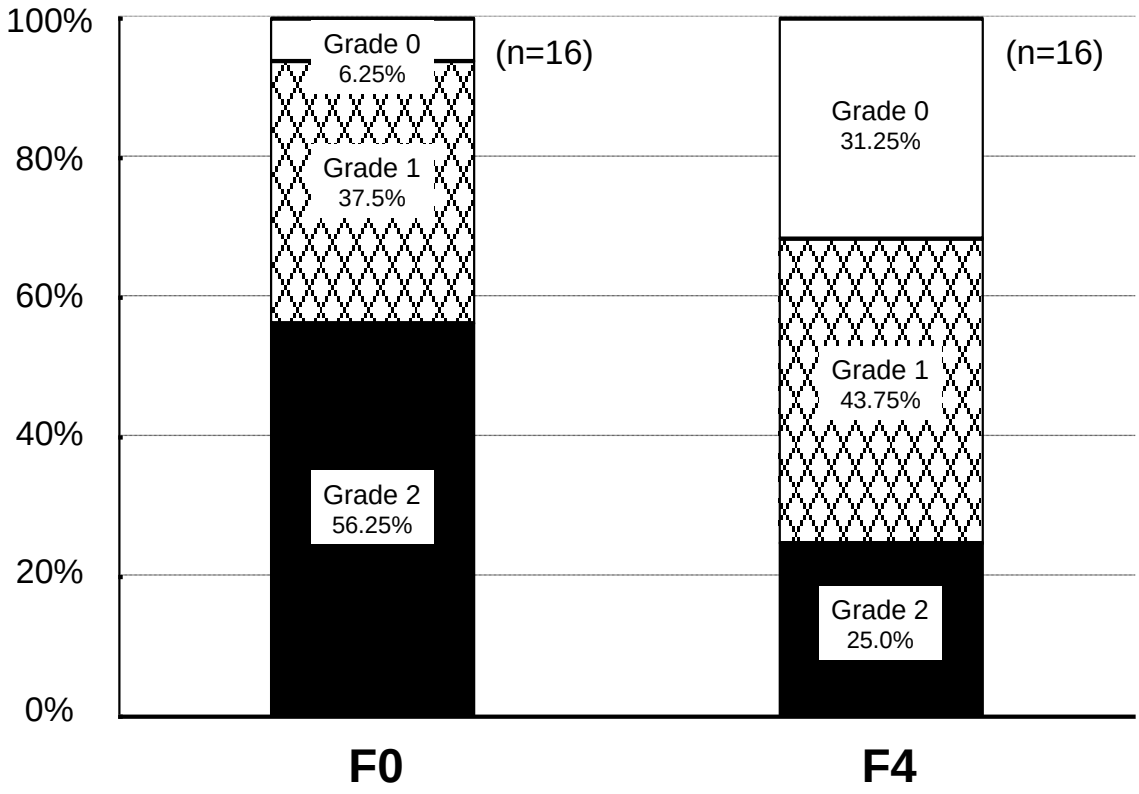

Figure 6.

Histological sections of a specimen in F4 screws with Grade 0 inflammation with the screw-skin interface remaining intact 4 weeks after operation, showing the presence of Sharpey's fiber-like tissue (H&E staining). b), c) and d) Magnified views of the boxed part in a). a) and b) Light microscopic image. c) and d) Polarized light microscopic images under crossed polar observation. d) View of c) after rotation at an angle of 34°.

A cell monolayer (arrow head) on the surface of the screw and many blood vessels (v marks) near the screw are seen (Fig. 6b). Crossed polar observation with the screw hole direction parallel to that of a polar demonstrated the interference color (white) of the aligned collagen fiber (Fig. 6c). Extinction of the interference color after rotation by an angle of 34° from the position in Fig. 6c (Fig. 6d) revealed that the direction of the aligned collagen fiber was 34° to the screw hole direction (black arrows in Figs. 6c and d).

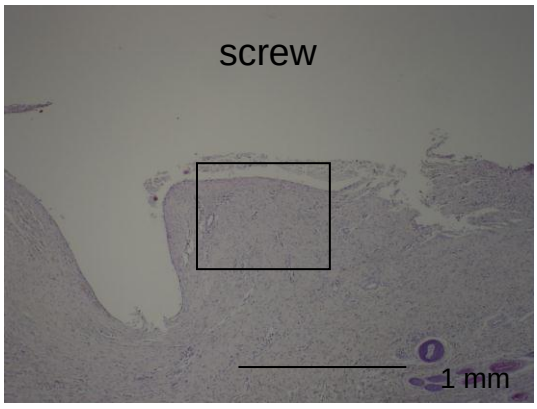

(a)

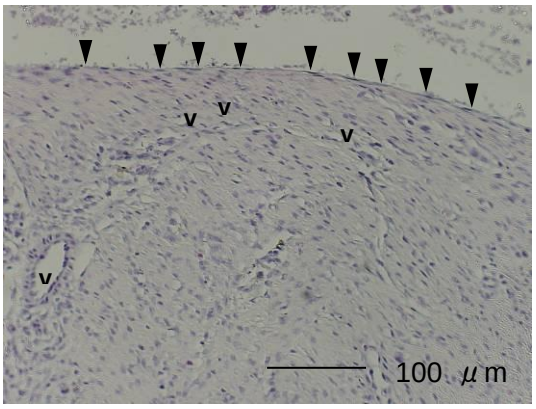

(b)

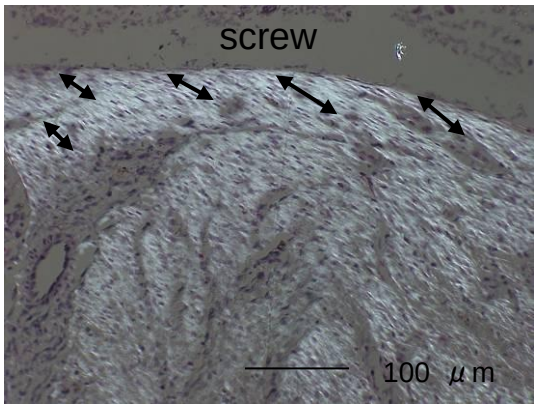

(c)

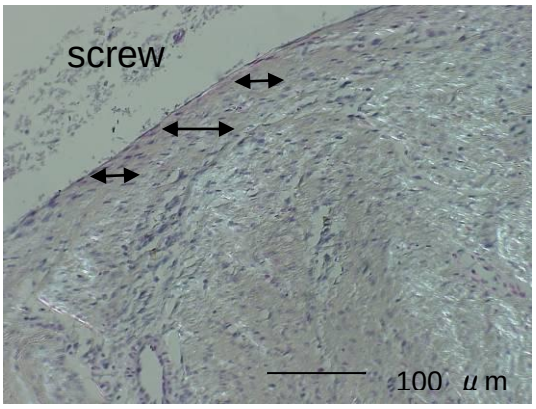

(d)

Figure 7.

Histological sections with Von Kossa staining of the specimen shown in Fig. 6. b) Magnified views of the boxed part in a). The Von Kossa's method stains a calcium salt brown. The direct adhesion of the thin cell monolayer to the FGF-2-apatite composite layer (brown) is visible.

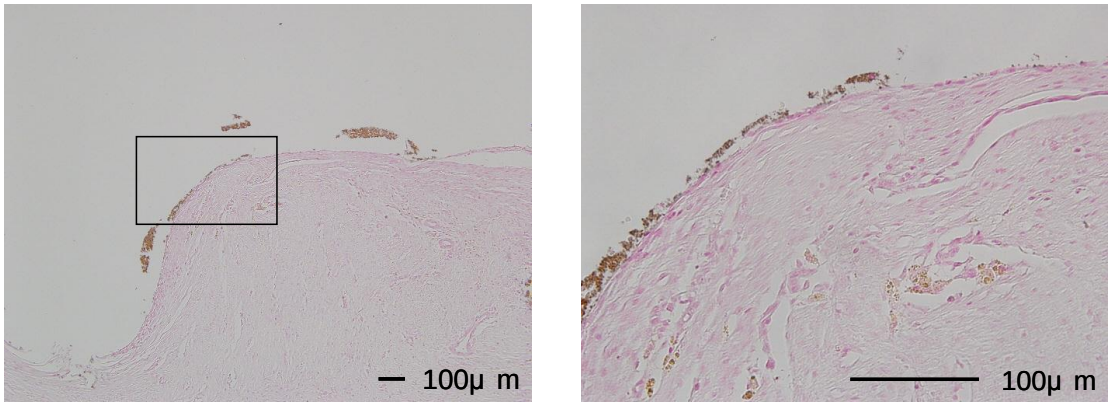

(a) (b)

Figure 8.

Histological sections of a specimen of F0 screws with Grade 0 inflammation with the screw-skin interface remaining intact 4 weeks after operations (H&E staining). b), c) and d) Magnified views of the boxed part in a). a) and b) Light microscopic image. c) and d) Polarized light microscopic images under crossed polar observation. d) View of c) after rotation at an angle of 45°.

A fibrous layer was observed around the screw surface (Fig. 8a and b). The fibrous layer was parallel to the screw (black arrow), which was observed in polarized light microscopy images (Fig. 8c and d). The formation of Sharpey's fiber-like tissue was not observed.

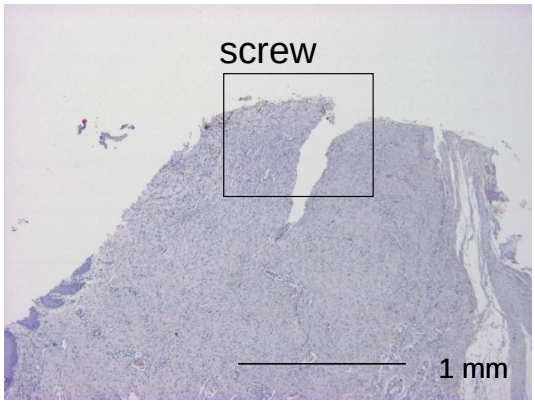

(a)

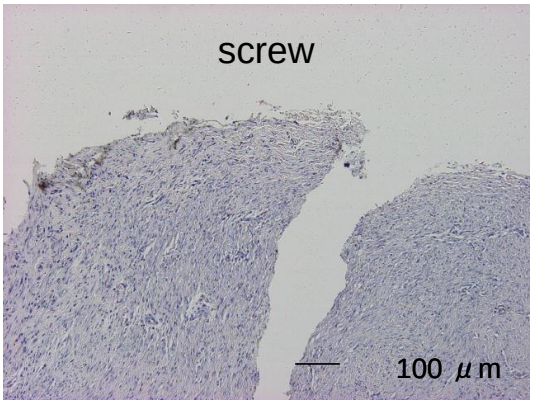

(b)

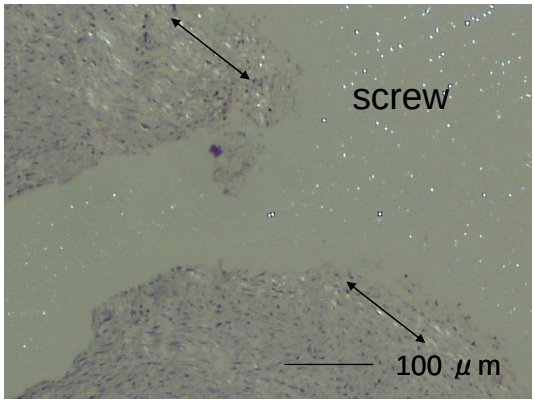

(c)

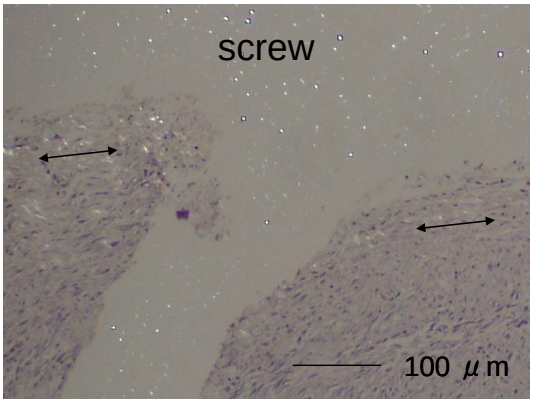

(d)